POAC'23
Glasgow, United Kingdom

Proceedings of the 27th International Conference on
Port and Ocean Engineering under Arctic Conditions
12-16 June 2023, Glasgow, United Kingdom

Ice drift and ice action on offshore wind farm structures

Helge Gravesen[1], Lars Bülow Jørgensen[1], Knut Vilhelm Høyland[2], Svend Bicker[3]
[1] Sweco (Offshore team, Copenhagen, Denmark)
[2] The Norwegian University of Science and Technology (NTNU) 7491 Trondheim, Norway.
[3] Deutsche Windguard Offshore GmbH

ABSTRACT

Development of offshore wind farms has so far been focused on areas without sea ice, but the increasing demand pushes the offshore wind industry into areas with seasonal sea ice, such as the Baltic Sea, the Great lakes and possibly the Bohai Sea. Sea ice is one of the major uncertainties and the present standards are insufficient. The international standard ISO19906 for arctic offshore structures is primarily prepared for large and relatively stiff quasi-static structures exposed to large ice driving forces. However, in most relevant cases for offshore wind farms the structures are far more flexible (dynamic) and the ice driving forces may be limited.

This paper will discuss load scenarios, when ice floes hit offshore wind turbine support structures and ice flow speed will reduce or stop by interaction with the support structures. The ice floes breaking mechanisms will be analysed related to the ice floe speed and relevant wind speed for the wind turbines. High ice loads will occur at low ice floe velocity in the range from 0 to 0.055 m/s due to intermittent crushing or frequency lock-in. In combination with wind speed (11 - 13 m/s) where the wind turbine operation shift from optimal power production to steady max power production high dynamic wind turbine loads can occur.

Analysis of data from projects in the South-eastern Baltic Sea have shown that there is a very low risk for occurrence of continuous limit stress scenarios simultaneously with critical wind speeds for the wind turbines in the range 11 - 13 m/s.

KEY WORDS: Drifting ice, Intermittent crushing, Windfarm,

INTRODUCTION

Wind turbines are very flexible (dynamic) structures where all structural elements and the control strategy is designed to avoid modal amplification. If the structure is exposed by a random load e.g. from sea ice the wind turbine control system may be incapable to regulate and high loads may occur. In this context it is important to assess the occurrence of high ice loads simultaneously with critical wind speeds for the wind turbine. This paper will discuss the scenarios of ice floe speed when the ice floe hit the wind turbine support structures. Figure 1 gives an overview of the assumed scenarios. We start by assuming the ice is forced by wind and current and is free drifting with a constant velocity. The free drift ice velocity is only a function of the wind and current velocities and the Nansen number (Na). Then the ice floe hit one foundation with a vertical wall in the waterline. When (if) the penetration reaches half the structure diameter (w_s) the floe slows down and one of three scenarios may occur, a) Steady-state crushing against one of several foundations, b) Floe stops or c) Ice cover deforms in ridging/rafting. We can identify three different forces, driving forces from wind and currents (F_d), ice crushing forces (F_s) and ridging forces (F_r) the two latter from ISO19906 (2019). The equations are derived below. While interacting with the foundation the ice velocity is a function of also the ice thickness (h_i), the ice area (A_i) and the ice load coefficient (C_R). Everything is based on Newton's second law, the ISO formulations for global pressure on vertical foundation and the ridging criterion as well as Stefan's law-type ice growth estimations (ISO19906, 2019).

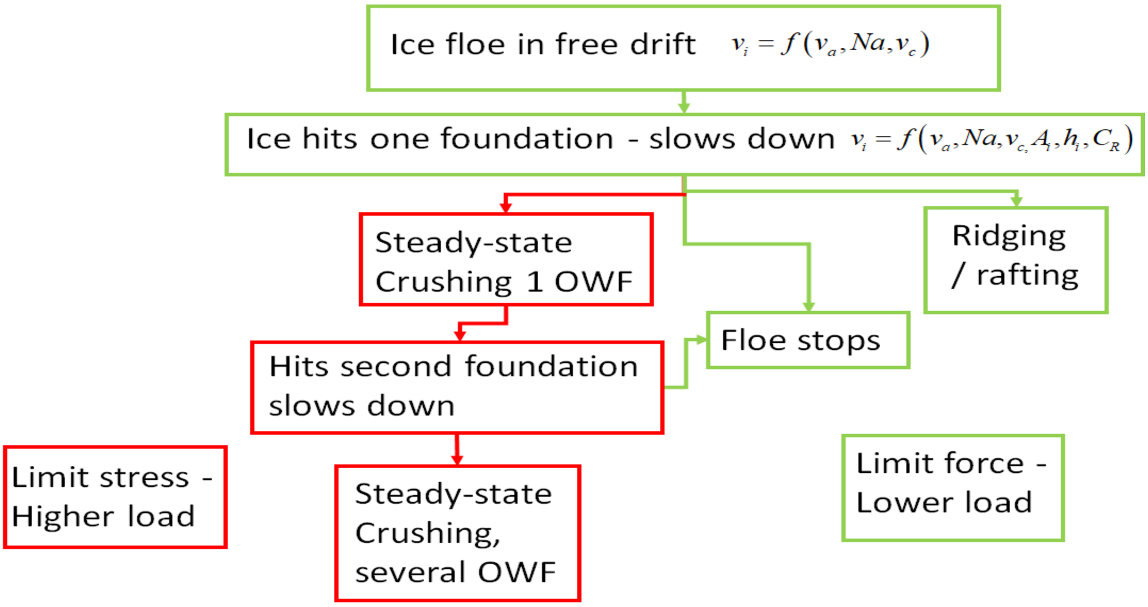

Figure 1. Overall scenarios (OWF: Offshore Wind Farm)

FREE DRIFT

The ice drift is often described by the equation of motion for a 2-dimensional continuous ice cover (Leppäranta, 2005). In this paper we have assumed "point masses" used a Lagrangian framework and applied Newton's second law directly. We further assume that we can neglect ice deformation, sea surface tilt, air pressure gradient and Coriolis' acceleration and finally assume that all vectors are parallel and that a positive current speed (v_c) is in the same direction as the wind speed (v_a), we can simplify and write:

$$\rho_i h_i A_i \frac{dv_i}{dt} = F_{air} - F_{current} = \frac{1}{2}\rho_a C_a A_i v_a^2 - \frac{1}{2}\rho_c C_c A_i \left(v_i - v_c\right)^2 \quad [1]$$

Where: ρ_i is ice density, h_i is ice thickness, A_i is ice area, ρ_a is air density, ρ_c is water density, C_a is air drag coefficient, C_c is current drag coefficients, v_a is wind velocity, v_c is current velocity and v_i is ice floe velocity. In free drift the velocity is constant, and we can find the ice drift velocity as a function of wind and current velocity:

$$v_i - v_c = \sqrt{\frac{\rho_a C_a}{\rho_c C_c}} v_a = Na \cdot v_a \qquad [2]$$

where Na is called the Nansen number, and v_a is mean wind velocity at 10 m altitude. The free flow ice drift velocity is often measured to be 2 - 3 % of the wind velocity (Na = 0.02 to 0.03).

STEADY-STATE CRUSHING

When the ice floe interacts with the wind turbine structure the ice velocity is reduced. To simulate this situation the ice crushing force term is added to Eq. 1. The structural response is not simulated, and we assume that the crushing force (F_s) is given by the global pressure formulation (p_G) in ISO19906 (2019).

$$\frac{1}{2}\rho_a C_a A_i v_a^2 - \frac{1}{2}\rho_c C_c A_i \left(v_i - v_c\right)^2 = F_s = p_G h_i w \qquad [3]$$

From this we can find ice drift velocity (assuming that $f_{AR} = 0$ and that $n = 0.3$):

$$v_i - v_c = \sqrt{\frac{\rho_a C_a}{\rho_c C_c} v_a^2 - 2 p_G \frac{h_i w_s}{\rho_c C_c A_i}} = \sqrt{Na \cdot v_a^2 - \frac{2 C_R h_i^{0.86} w_s^{0.84}}{\rho_c C_c A_i}} \qquad [4]$$

Narrow structures or thin ice gives a bit more complicated but still trivial formulas and these were applied whenever valid. Both Hendrikse and Koot (2019) and Hendrikse and Nord (2019) has done similar calculations of equilibrium ice drift speed.

ICE FLOW SLOWING DOWN

To evaluate the stopping period for the ice floe movement Newton's second law over the ice floe penetration length (u) is applied:

$$\int_{u_0}^{u_1} (F_a - F_s) du - \int_{u_0}^{u_1} \left(F_c(v_i)\right) du = \int_{u_0}^{u_1} \left(m_i a_i\right) du \qquad [5]$$

If we assume that the ice floe is so large that the ice area (A_i) is constant, the only changing variable is the ice floe velocity and we can find:

$$(F_a - F_s)\left(u_1 - u_0\right) - \frac{1}{2}\int_{u_0}^{u_1} \left(\rho_c C_c A_i (v_i - v_c)^2\right) du = \frac{1}{2} m_i \left(v_{i,1}^2 - v_{i,0}^2\right) \qquad [6]$$

Assuming that ice velocity is constant during one time step:

$$\left(u_1 - u_0\right) = v_0 \Delta t \qquad [7]$$

we obtain an expression for ice velocity and time step:

$$\sum F \cdot v_0 \Delta t = (F_a - F_c - F_s) v_0 \Delta t = \frac{1}{2} m_i \left(v_{i,1}^2 - v_{i,0}^2 \right) \quad [8]$$

where F_a, F_c and F_s are given in Eqs. 1 and 4. The ice velocity in time step j becomes:

$$v_{i,j}{}^2 = \frac{2(F_a - F_c - F_s) v_{i,j-1} \Delta t}{m_i} + v_{i,j-1}^2 \quad [9]$$

RIDGING AND RAFTING

In this section it will be evaluated whether ridging or rafting will occur instead of ice crushing as assumed in the previous sections. The condition for ridging/rafting is that the driving forces are larger that ice ridging criterion (F_{ri}) and at the same time the ridging force is less than ice crushing force (F_s) given in Eq.10. The force required to ridge is given in Eq. 11 (ISO19906, 2019).

$$F_d > F_{ri} < F_s \quad [10]$$

$$F_{ri} = w_i \cdot R \cdot h_i^{1.25} \cdot w_i^{-0.54} = R \cdot h_i^{1.25} \cdot w_i^{0.46} \quad [11]$$

where F_{ri} is given in [MN], R is an empirical factor from 2 - 10, w_i is the width of the floe given in meters and h_i is the level ice thickness also given in meters (ISO19906, 2019). The two inequalities in Eq. 10 give Eqs. 12 and 13 (for simplicity we assume that f_{AR} = 0 and that n = 0.3 (h_i > 1m)).

$$w_i < \left[\frac{C_R}{R} h_i^{-0.39} w_s^{0.84} \right]^{2.17} \quad [12]$$

$$A_i = l_i w_i > \frac{2 h_i w_s}{\rho_a C_a} \frac{p_G}{v_a^2} \quad [13]$$

It is found by Eqs. 12 and 13 that ridging or rafting only will occur for a long and narrow ice floe. If several foundations are blocking the ice floe moment the probability of ridging or rafting increases and at the same time the probability of crushing decreases (F_s increases with increasing number of foundations). There are no data available on ridges in the South-eastern Baltic and it is rather possible that rafting is more probable as the ice is thin and smooth (often with a little snow cover). However, the probability of ridging or rafting will be very low in our case.

ICE THICKNESS ESTIMATIONS

The ice thickness is estimated from Freezing Degree Days (*FDD)* as given in below (Eq. 14)

$$h_i = 0.024 \sqrt{(0.9 \cdot FDD - 50)} \quad [14]$$

This formulation is a modification of the Danish rules that are calibrated for open waters based on data in Danish water since the 1940s. Our current case is more of an offshore location so that the one of the factors was reduced from 0.03 to 0.024.

ICE BREAKING MECHAMISMES VS. FLOE SPEED

Based upon analysis of the ice drift toward the Nordströmsgrund lighthouse the ice breaking mechanisms are separated in three regimes: Intermittent crushing, frequency lock-in and continuous brittle crushing ref. Figure 2. The floe speed that will generate highest loads by intermittent crushing or frequency lock-in is found in the range 0 – 0.055 m/sec (Figure 2 and Figure 3).

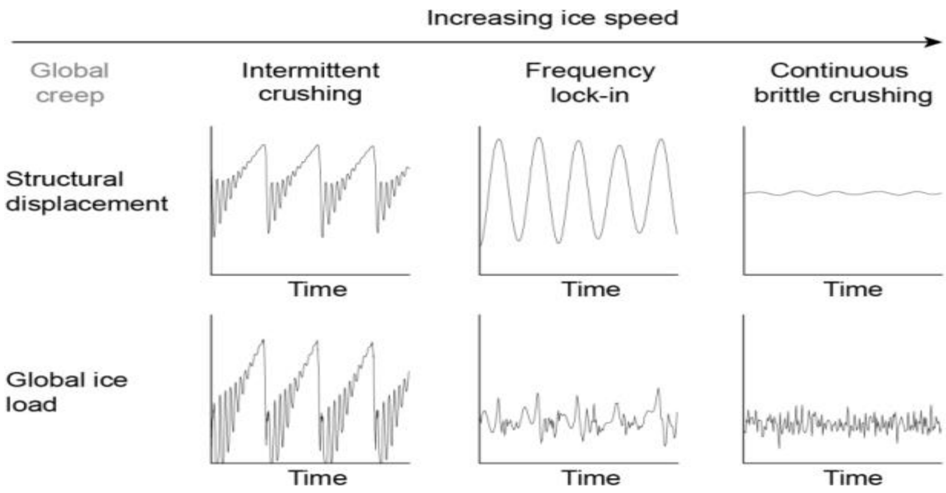

Figure 2 Illustration of the structural displacement at the ice action point and the global ice loads in the three regimes of ice breaking mechanisms and induced vibrations.

The Nordstömsgrund light house is considered as a rigid structure where the structural frequencies do not overlap with the lock-in frequency of the ice crushing therefor amplification of the structural displacement do not occur. In contrast to the lighthouse a wind turbine support structure is a flexible structure supporting a rotating rotor with several bending modes and damping mechanisms. It will be needed to investigate the consequences of the dynamic ice load impact in combination with the wind turbine dynamic.

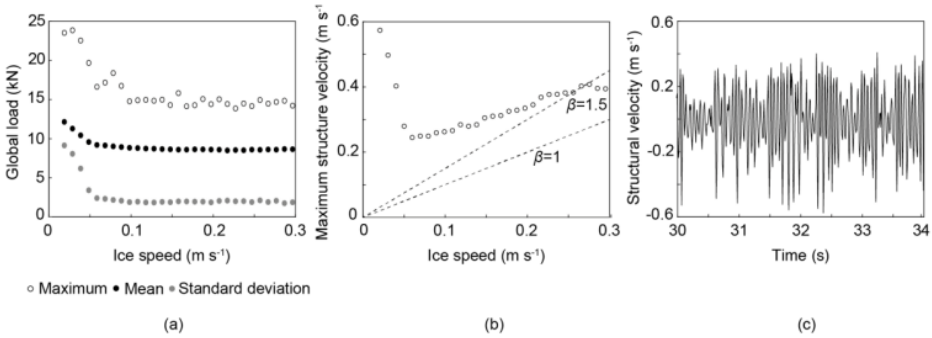

Figure 3 Results from experiments carried out by HSVA, DIIV campaign. (a) Simulated measures of global load, (b) Simulated peak velocity amplitude of the structure. (c) Simulated structural displacement at the ice action point for an ice drift speed of 0.28 m/s. Määttänen M., et.al. (2012).

SIMULATIONS

Based on the methods and equations Eqs. 1 – 14 defined in the first sections of this paper following parameters are used for the simulations: Wind speed: 0 - 25 m/s, Current speed: 0 - 0.5 m/s, Ice floe size: 1 km x 1 km – 1 km x 10 km, Width of support structure: 9 m, C_R crushing strength: 0.66 MPa (2009) and two ice thickness's h_{50} and $h_{50}/2$ that represent a 50 year return period value and the half here off.

For this set of input parameters, the ice floe speed is found for 4 scenarios of ice floe speed: 0, 0.055, 0.2 and 0.5 m/s. The ice floe speed interval 0-0.055 m/s is critical since high ice loads and dynamic (intermitted crushing) occur in this region. The ice floe speeds of 0.2 and 0.5 m/s are included to illustrate the scenario for faster moving ice (brittle crushing).

For the wind turbine the critical wind speeds is in the range 11-13 m/s at hub height where high loads can occur during power regulation. In this range the trust load on the wind turbine rotor is high and the regulation regime shift from optimal power output to regulated power output. A wind shear factor of 1/1.25 is used between the wind speed at hub height to the wind speed acting on the ice surface.

The used wind speed and current floe speeds are corelated to hindcast data for an offshore wind farm location in the South-eastern Baltic Sea to evaluate the compliance with site specific data.

STEADY-STATE ICE DRIFT WHILE CRUSHING AGAINST A STRUCTURE.

Firstly, we apply the equations [1] – [4] with the parameters as described above and find the steady-state ice drift speed with ice-structure interaction as a function of wind speed, current speed, floe size and ice thickness. Only plots of ice thickness h_{50} and $h_{50}/2$ and floe size 1 km x 5 km and 1 km x 10 km are included below.

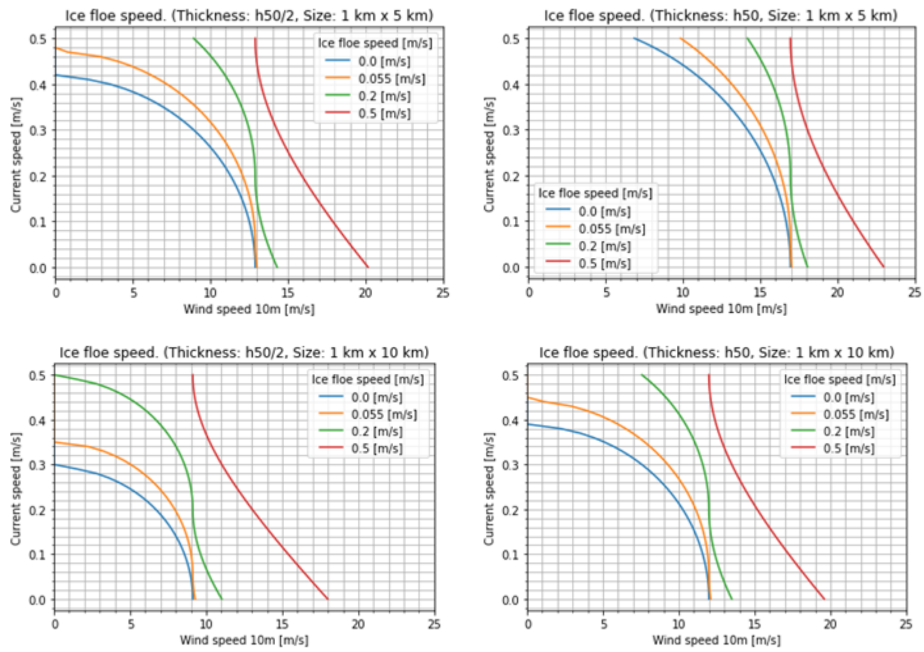

Figure 4 Contour plot of the equilibrium drift speed as a function of the wind and current speed for an ice thickness of h_{50} and $h_{50}/2$ an ice floe length of 5 km and 10 km.

Figure 4 shows that the ice floe speeds 0 – 0.055 m/s only occur in a narrow band (between the blue and orange lines) with the right combination of wind and current speed. It can also be seen that the ice floe with the lowest thickness will move for a lower combination of wind and current speed compared to a thicker ice. This is due to the fact that the surface of the ice floe is the same but the resistance from the foundation is less due to lesser ice thickness.

In Figure 5 and Figure 6 the ice drift velocities of 0 m/s and 0.055 m/s are illustrated for different ice thicknesses and the situations for an ice covered area of respectively 1 km x 5 km and 1 km x 10 km. These figures also include hindcast wind and current speed data in the period 1979-2019 where sea ice had occurred for a typical location in the South-eastern Baltic Sea.

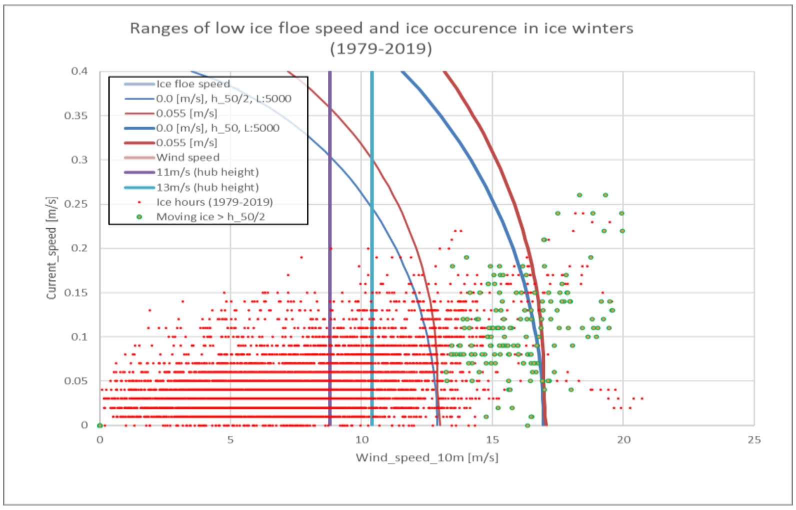

Figure 5 Ranges of ice floe speed 0 and 0.055 m/s for two ice thickness h_{50} and $h_{50}/2$ for an ice-covered area of 1 km x 5 km and one hourly occurrence (dots) of wind speed and current speed during sea ice occurrence in the winters from year 1979 to year 2019. The two vertical lines at 8.8 and 10.4 [m/s] (10m) indicate the wind speeds for the wind turbine in the regulation range 11 to 13 [m/s] (hub height). Green dots illustrate that the ice floe in the range $h_{50}/2$ – h_{50} thickness will move after hitting the foundations.

It can according to Figure 5 be seen that if the ice-covered area is 1 km x 5 km very few moving ice occurrences are found for the ice thickness range $h_{50}/2$ to h_{50} in the 0 – 0.055 m/s ice speed range. The critical wind speed regime for the wind turbine is from 11- 13 m/s (at 10 m: 8.8-10.4 m/s) (the regulation regime) and it can be seen that > $h_{50}/2$ ice occurrences are outside this wind speed regime.

In Figure 6 the situation for an ice-covered area of 1 km x 10 km is illustrated.

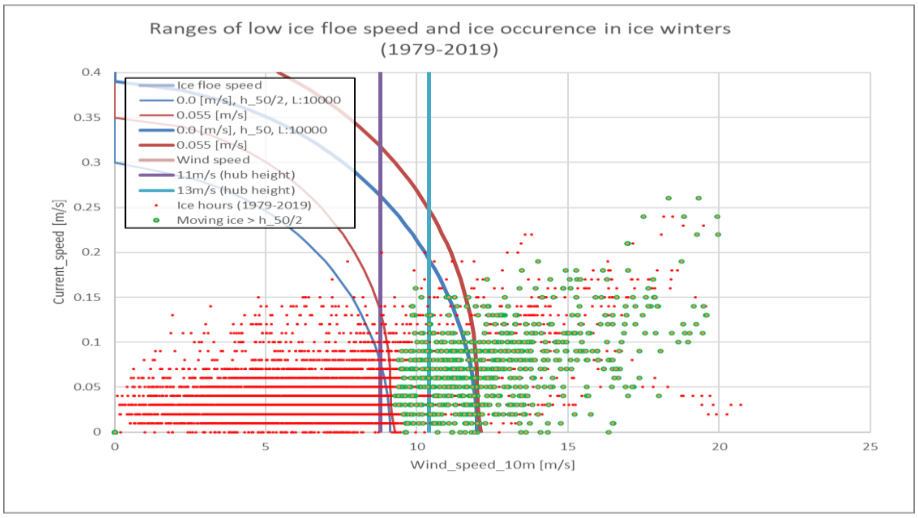

Figure 6 Ranges of ice floe speed 0 and 0.055 m/s for two ice thickness h_{50} and $h_{50}/2$ for an ice-covered area of 1 km x 10 km and one hourly occurrence (dots) of wind speed and current speed during the ice periods in winters from year 1979 to year 2019. The two vertical lines at 8.8 and 10.4 m/s (10m) indicate wind speeds for the wind turbine in the regulation range 11 to 13 m/s (hub height). Green dots illustrate that the ice floe in the range $h_{50}/2 – h_{50}$ thickness will move after hitting the foundations

According to Figure 6 it can be seen that if the ice covered area is 1 km x 10 km during an extreme ice winter an overlap occur of wind speed in the range 8.8 – 10.4 m/s and moving ice thicker than $h_{50}/2$ with a floe speed between 0 and 0.055 m/s. This can also be illustrated by Figure 7 that show the ice flow speed vs. wind speed.

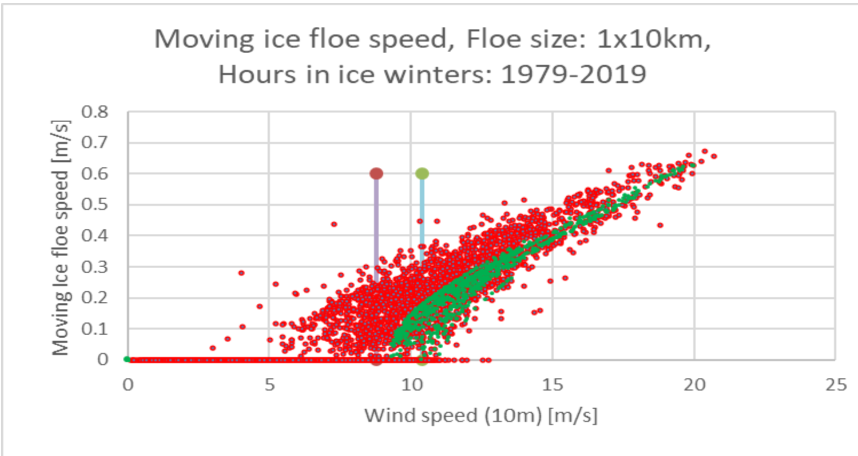

Figure 7 Moving ice floe speed for an ice covered area of 1 km x 10 km vs. wind speed. The two vertical lines mark the wind speed range 8.8 – 10.4 m/s. The red and green dots mark the 1 hour occurrences of sea ice where the green dots are for ice thickness in the range $h_{50}/2$ to h_{50} in the years 1979 -2019.

Figure 8 is a zoom of Figure 7 the region wind speed 8 - 11 m/s and ice floe speed 0 - 0.055 m/s.

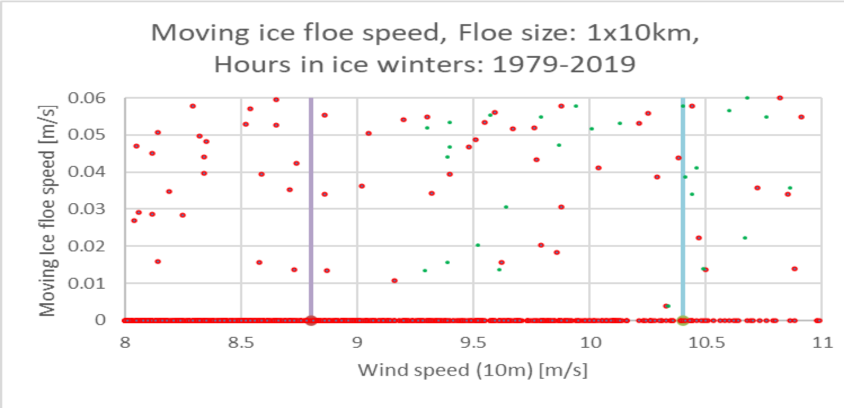

Figure 8 Zoom of Figure 7 for wind speed 8.6 – 10.4 m/s and ice floe speed of 0 – 0.055 m/s. Totally 14 hours (green dots) of ice movement is found in this region.

It can be concluded that in the period 1979 – 2019 the number of occurrences of low ice velocity (0 - 0.055 m/s) and wind speed in the region 8.8-10.4 m/s (11-13 m/s at hub height) is low. The ice covered area shall be large (1 km x 10 km) and the floe shall hit a single foundation before the scenario as shown in Figure 7 and Figure 8 apply.

ICE FLOE STOPPING TIME

When the ice floe moves freely it is exposed to interaction from the wind and current. When the ice floe hits a wind turbine support structure the ice floe will slow down or stop depending on the external forces. Considering the work balance derived by Eqs. 5 – 9 the stopping time, defined as the time from when the ice floe first hits the structure until it is at rest, can be calculated.

The stopping time as a function of current speed is shown for different wind speeds, ice thickness and ice floe sizes in Figure 9. The current is illustrated for the situations where it is working in the same direction as the wind speed (positive current) and the situation were in is working in the opposite direction (negative current). The current not in line with the wind is not considered.

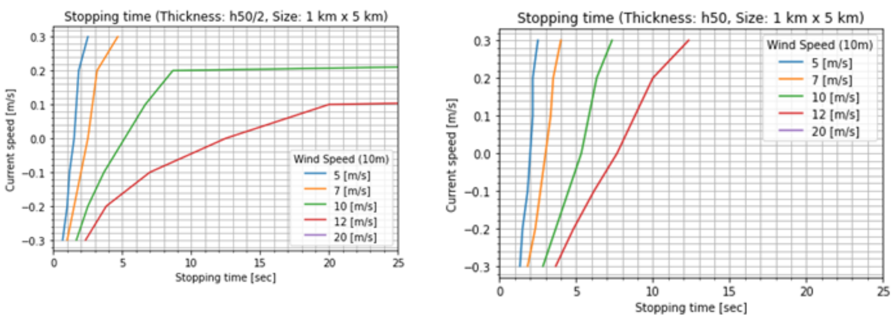

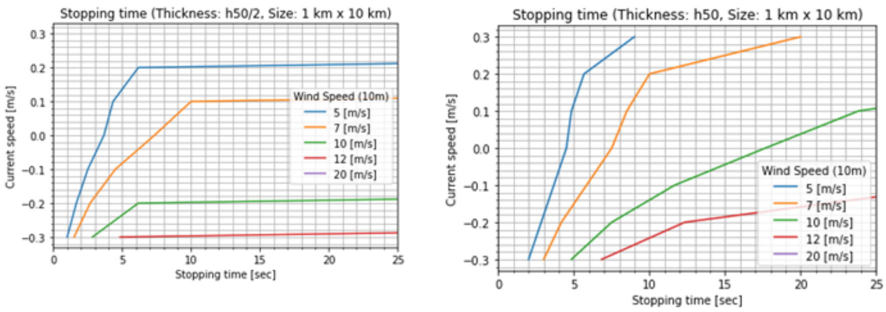

Figure 9 Ice floe stopping time as function of the wind and current speed for an ice thickness of $h_{50}/2$ and h_{50} an ice floe length of 5 km and 10 km.

CONCLUSION

For the South-eastern Baltic Sea it is concluded that the ice floe primarily will crush at the structure and that ice rafting or generation of ice ridges are unlikely to happen. It is found that the occurrence of ice floe speed (0 - 0.055 m/s) that might cause intermittent crushing or frequency lock-in for Offshore Wind Turbines OWTs in the South-eastern Baltic Sea is extremely low.

The analysis of the load balance (driving force from wind and current and resistance from the foundations) show that the critical ice flow speed (0 - 0.055 m/s) only occurs in a narrow band with the right balance of wind, current and resistance from the foundation and that the overlap with critical wind speed (11-13 m/s at hub height) for the wind turbine is very limited. The analysis of the work performed during ice floe crushing at the foundations show that the foundation will provide a considerable resistance to the ice flow speed and stop the movement of the ice floe within few seconds in most cases especially for the wind speed critical range (11-13 m/s at hub height).

When using site related data it is found that in total 14 hours are found in the critical ice floe range 0-0.055 m/s (actual range is 0.015 m/s to 0.055 m/s) and $h_{50}/2 – h_{50}$ ice thickness which over a period of 40 year (1979-2019) is considered being extremely low. The total amount of hours during which ice is present are 7104 hours out of which only 644 hours show moving ice. In the remaining situations the ice is stopped by interaction with the foundations. Hence the probability of ice velocities in critical thickness range $h_{50}/2 – h_{50}$ is $14/7104 = 1.97*10^{-3}$.

The situation with the 1 km x 5 km and 1 km x 10 km floe size will be very rare in the South-eastern Baltic Sea. According to the German Ice Atlas, BSH (2012) the longest period of total ice coverage at the area north of Poland was observed in year 1963 from 1st March to 11th March = 10 days.

If this situation is considered as the 50 years return period extreme ice situation, it can conservatively be assumed that the 1 km x 10 km ice floe will appear for maximum 10 days. Probability: $10/(50*365) = 5.5*10^{-4}$. Combining these two uncoupled probabilities gives: $1.97*10^{-3} * 5.5*10^{-4} = 1.08*10^{-6}$ which is equivalent to 28 minutes per 50 years. If the directional distribution of the wind and current is included the probability is further reduced.

The wind farm structures will be place in a grid where only the first row of structures toward open water will be exposed to the largest ice floes. The structures in the internal rows in the wind farm(s) will be protected by the first rows of structures.

REFERENCES

ISO19906, 2019. Petroleum and natural gas industries - Arctic offshore structures. *Tech. rep., International Standard, International Standardization organization, Geneva, Switzerland*, 568 p.

Leppäranta, M., 2005. The drift of sea ice. *Springer-Praxis, Springer-Verlag Berlin Heidelberg New York,* ISBN 3-540-40881-9, 266 p.

Høyland, K. V., 2023 Note on Ice drift and ice actions on OWF + personal communication

Høyland, K.V., Nord, T.S., Hendrikse, H., Tuhkuri, J., Polojärvi, A., von Bock und Polach, F., Heinonen, J. Eik, K.J., Teigen, S.H., Serré, N., Schümann, B., von Borstel, T., Reimer, N., Haase, A., and Sjöblom, A., 2023. Challenges with sea ice action on structures for Offshore wind *Proceedings of the 27th International Conference on Port and Ocean Engineering under Arctic Conditions, Glasgow, Scotland, 2023, paper 98..*

BSH, 2012. Bundesamt für Seeschifffahrt und Hydrographie, "Climatological Ice Atlas for the Western and South-eastern Baltic Sea (1961-2010).

Hendrikse, H and Koot,J., 2019. Consideration of ice drift in determining the contribution of ice induced vibrations to structural fatigue, in *Proceedings of the 25th International Conference on Port and Ocean Engineering under Arctic Conditions, Delft, The Netherlands*, June 9-13, 2019.

Hendrikse, H. and T. Nord, T., 2019. Dynamic response of an offshore structure interacting with an ice floe failing in crushing. *Marine Structures,* vol. 65, pp. 271-290, 2019.

Määttänen M, Løset S, Metrikine A, Evers K-U, Hendrikse H, Lønøy C, Metrikin I, Nord T, and Sukhorukov S., 2012. Novel ice induced vibration testing in a large-scale facility. Deciphering ice induced vibrations, part 1. Proceedings of the 21st IAHR International Symposium on Ice. p. 946–58. [Dalian, China].

Gravesen, H. and Kärnä, T., 2009. Ice Loads for Offshore Wind Turbines in Southern Baltic Sea. June *Proceedings of the 20th International Conference on Port and Ocean Engineering under Arctic Conditions, Luleå, Sweden. Paper #3.*